Electrostatic Free Energy Calculations for Macromolecules: A Hybrid Molecular Dynamics/Continuum Electrostatics Approach

Thomas Simonson

Laboratoire de Biologie Structurale, Institut de Génétique et Biologie Moléculaire et Cellulaire (CNRS), 1 rue Laurent Fries, 67404 Strasbourg-Illkirch, France

Received: April 14, 2000; In Final Form: May 15, 2000

A hybrid molecular dynamics/continuum electrostatics method is proposed for free energy calculations that involve the creation or deletion of net charges in a solvated macromolecule, which extends and simplifies an earlier method. A limited, spherical region of interest is treated microscopically; the remainder of the system is treated as a heterogeneous dielectric continuum. The spherical region contains part of the macromolecule and a limited number of explicit solvent molecules, while the outer region contains the remainder of the macromolecule and bulk solvent. In a first step, the dielectric constant of the macromolecule in the outer region is changed from a value typical of the macromolecule (∼1−4 for a protein) to a value typical of a bulk solvent. Second, the mutation is introduced with a molecular dynamics simulation for the spherical region, including the reaction field due to the now-homogeneous outer region, for which analytical expressions are available. Third, the outer macromolecular dielectric constant is changed back to its original value. The free energies for steps one and three are obtained from continuum electrostatics. The method is used to calculate the free energy to mutate a negatively charged aspartate ligand into a neutral asparagine in the active site of aspartyl-tRNA synthetase and shown through comparison to the earlier method to be efficient and accurate.

Introduction

The calculation of free energy changes for electrostatic processes in macromolecules such as proteins is of fundamental importance for understanding their structure and function.[1,2] Electrostatic interactions play an important role, for example, in enzyme transition state stabilization, in oxidation−reduction processes, in the pH-dependent ionization of acidic and basic groups, and in molecular recognition. The most fundamental approach to this problem has been to use molecular dynamics simulations of a solvated macromolecule in combination with thermodynamic perturbation theory.[3−5] This approach allows local transformations to be studied, such as point mutations in a protein, proton binding at a titratable site, or oxidation of a chromophore. For the method to be successful, it is imperative that long-range electrostatic interactions be treated accurately. One method is to simulate the fully solvated macromolecule with periodic boundary conditions and treat the long-range interactions by Ewald summation.[6,7] For a large protein, this is very expensive because of the quantity of explicit solvent required, and there are no examples of such free energy calculations for proteins in the literature so far. In the application below, for example, a model with 50 000−100 000 atoms would be needed, instead of the ∼6000 used here. Another method is to treat bulk solvent with a continuum reaction field[8,9] or a Langevin dipole approximation.[1,4] If the explicit solvent region is large, the cost is again very high, as with the Ewald method. If it is small, the continuum reaction field problem is not spherically symmetrical (see Figure 1) and a large computational overhead arises.[10,11] Only a few examples exist in the literature, all using Langevin dipoles; see e.g. refs 1 and 4.

An alternative is to introduce the mutation of interest with a finite simulation model including a limited number of explicit solvent molecules, then calculate the free energy to transfer the finite model to and from bulk solvent with a continuum model.[12,13] This method was used to study the mutation of a negatively charged aspartate ligand (Asp) into a neutral asparagine (Asn), in the active site of the protein aspartyl-tRNA synthetase (AspRS) and shown to be efficient and accurate for that system.[13] However, it uses a transfer of the macromolecule between bulk solvent and a phase where only a few hundred waters are present. There could be significant structural changes during such a transfer, e.g., for solvent close to the surface; in particular, artificially high pressure and density have been observed in simulations with finite models.[14] The continuum electrostatics model used to calculate the transfer free energy assumes that structural changes during this step are not too large, so that a linear response approximation is valid. While this condition was satisfied in the application reported,[13] it could be violated for other systems. The method proposed below requires a weaker structural assumption. It surrounds the model by bulk solvent in the MD step, so that the internal pressure and density should be more realistic. As a test problem, we consider the same Asp → Asn mutation in the AspRS active site. The Asp → Asn mutation in solution has been studied elsewhere.[15]

Methods

The method proceeds as follows. The system is divided into two regions: an "inner" region centered on the group being mutated, containing part of the macromolecule and a limited number of explicit solvent molecules, and an "outer" region, containing the rest of the macromolecule and bulk solvent (see Figure 1). The inner region has an approximately spherical shape. It will be treated using microscopic simulations such as molecular dynamics (MD), while the outer region will be treated as a heterogeneous dielectric continuum. The mutation is performed in three steps. In step I, the dielectric constant of

10.1021/jp0014317 CCC: $19.00
Published on Web 06/24/2000

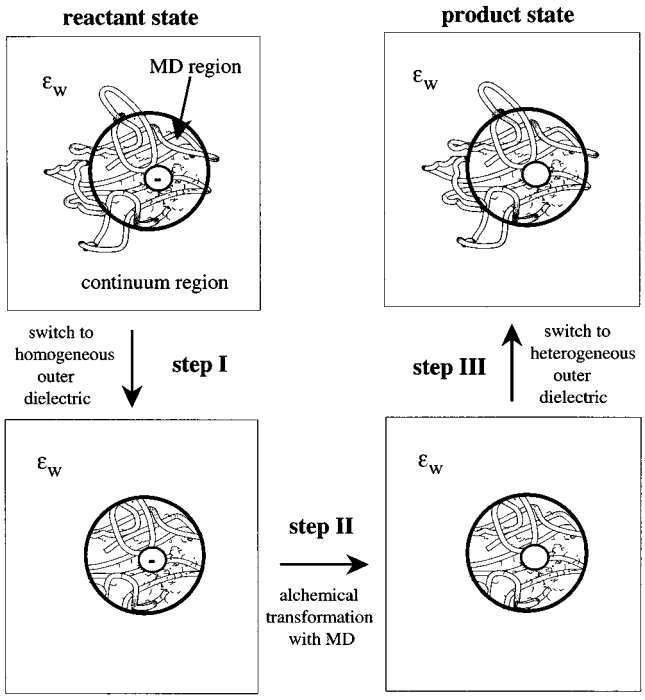

Figure 1. Three-step pathway to compute the free energy change ΔG associated with a local transformation in a macromolecule in bulk solution. Step I: the dielectric constant of that portion of the macromolecule that lies outside a spherical inner region ("MD region") is switched to that of bulk solvent. Step II: the local transformation is carried out using a series of molecular dynamics simulations. In the present application, an Asp → Asn mutation is performed in an enzyme active site; the transformation is schematized by the removal of a − sign near the center of the inner, MD region. Step III: the dielectric constant of that portion of the macromolecule that lies outside the MD region is switched back to its original value (1 in the present study). The free energy changes for steps I and III are calculated with a Poisson−Boltzmann continuum model; the free energy change for step II is calculated from thermodynamic perturbation theory.

that portion of the macromolecule that lies in the outer region is changed to the bulk solvent value. The corresponding free energy is calculated from continuum electrostatics. During this step, the inner region is treated as a low-dielectric cavity containing point charges located on each atom. In step II, the mutation is introduced using molecular dynamics (or Monte Carlo) simulations; the free energy change is obtained from standard thermodynamic perturbation theory.[3,4] In this step, the dielectric constant of the outer region is uniform and equal to that of bulk solvent. This makes it straightforward to include the reaction potential from the outer region in the MD simulation. Indeed, with a single, spherical, dielectric interface, analytical solutions are available for the reaction potential, which are implemented in many molecular dynamics packages (see, e.g., refs 8 and 9). In step III, the dielectric constant of that portion of the macromolecule that lies in the outer region is changed back to the value appropriate for the macromolecule, with the solute in the product state (i.e., after the mutation). The free energy for this step is calculated from continuum electrostatics, as in step I. For the continuum electrostatics steps I and III, standard finite-difference methods can be used,[16] which solve the Poisson or Poisson−Boltzmann equation numerically, and results can be averaged (as below) over multiple conformations of the reactant and product states. The overall process is schematized in Figure 1.

It is expected that in many applications, the partial charges of the solute atoms that lie outside the spherical MD region can be neglected. In that case, the outer portion of the solute contributes to the free energy only by excluding high-dielectric solvent. This approximation is adopted here, but it is not essential to the method. For the system studied below, the outer charges were shown earlier to contribute negligibly,[13] because they are more than 24 Å away from the mutation site and because they are largely shielded by continuum solvent. The same is expected to hold for other systems, as long as the inner, MD region is of comparable size and the solvent content of the outer region is not too low.

To obtain the free energy change ΔG_{II} for the microscopic simulation step II, the contribution of the reaction potential must be included. To do this, the potential energy function must be replaced by a potential of mean force $W(r_1,r_2,...,r_n;\lambda)$,[9,17] which depends on the coordinates r_i of the atoms in the inner region and on a coupling constant λ that describes the progress of the mutation.[3,5,13] The configurational part of the classical mechanical partition function has the form

$$Q(\lambda) = \int \exp(-W(r_1,r_2,...,r_n;\lambda)/kT)\, dr_1...dr_n \qquad (1)$$

where k is Boltzmann's constant and T is the absolute temperature. Thus

$$\frac{\partial \Delta G_{II}}{\partial \lambda} = \left\langle \frac{\partial W}{\partial \lambda} \right\rangle_\lambda \qquad (2)$$

where the brackets indicate an average over the (V, T) or the (p, T) ensemble with a coupling constant of λ. With a continuum electrostatics model of the outer region, the potential of mean force (pmf) contains two contributions: the potential energy function U for the inner region and a contribution ΔW from the continuum solvent:[9,17]

$$W(r_i;\lambda) = U(r_i;\lambda) + \Delta W(r_i;\lambda) = U(r_i;\lambda) + \frac{1}{2}\sum_{j\in \text{inner}} q_j(\lambda)\, V_j^{\text{reac}}(r_i;\lambda) \qquad (3)$$

The sum in the second term is over all partial charges q_j in the inner region; V_j^{reac} is the reaction potential produced by the outer continuum at r_j. The "solvation potential" ΔW is the free energy to "charge up" the inner region (i.e., to introduce the charges q_j) in the presence of the continuum solvent, minus the free energy to charge it up in a vacuum (in the same spatial configuration $\{r_j\}$).[9,17]

To exploit eqs 2 and 3, we assume the transformation deletes a certain set of charges (the set C), creates others (set B), and leaves others unchanged (set A), and we adopt the linear coupling scheme:

$$\text{if } j \in A,\ q_j(\lambda) = q_j^0$$

$$\text{if } j \in B,\ q_j(\lambda) = \lambda q_j^0$$

$$\text{if } j \in C,\ q_j(\lambda) = (1-\lambda) q_j^0 \qquad (4)$$

where λ is varied from 0 to 1. In the application below, an aspartate side chain is deleted while an asparagine side chain is created. Thus, C is the set of Asp side chain charges, B the set of Asn side chain charges, and A the set of all remaining charges within the spherical MD region, including ligand backbone, protein and solvent. In this application, the transformation also involves nonelecrostatic energy terms treated by standard

methods described further on. Expressing the reaction potential as a sum over all the source charges q_j and grouping terms according to their λ-dependency, we obtain

$$\Delta W(r_i;\lambda) = \frac{1}{2}\sum_{i,j\in A} q_i^0 q_j^0 V_{i\to j} + \frac{\lambda^2}{2}\sum_{i,j\in B} q_i^0 q_j^0 V_{i\to j} + \frac{(1-\lambda)^2}{2}\sum_{i,j\in C} q_i^0 q_j^0 V_{i\to j} + \sum_{i\in A,j\in B} \lambda q_i^0 q_j^0 V_{i\to j} + \sum_{i\in A,j\in C} (1-\lambda) q_i^0 q_j^0 V_{i\to j} + \sum_{i\in B,j\in C} \lambda(1-\lambda) q_i^0 q_j^0 V_{i\to j} \quad (5)$$

Here, $V_{i\to j}$ is the reaction potential at r_j when a unit charge at r_i is the only source charge present (i.e., the Green's function), and the reciprocity relation $V_{i\to j} = V_{j\to i}$[18] has been used. We obtain finally

$$\frac{\partial \Delta W}{\partial \lambda} = \Delta W^0_{AB} - \Delta W^0_{AC} + (2\lambda - 1)(2\Delta W^0_{BB} + 2\Delta W^0_{CC} - \Delta W^0_{BC}) \quad (6)$$

where ΔW^0_{XY} is the value of the solvation potential ΔW when only the charges q_i^0 in sets X and Y are present (X, Y = A, B, or C); e.g.

$$\Delta W^0_{AB} = \frac{1}{2}\sum_{i,j\in A\cup B} q_i^0 q_j^0 V_{i\to j} \quad (7)$$

The first two terms on the right of (6) couple the ligand side chains (sets B, C) to their environment (set A) through the surrounding dielectric continuum. The third term couples the side chains B and C to themselves and to each other. In most applications, the mutated groups will be near the center of the sphere, with limited mobility, so that ΔW^0_{BB}, ΔW^0_{CC}, and ΔW^0_{BC} will change little as a function of time and λ; thus the last term will have approximately the form $(2\lambda - 1) \times$ constant, and an integral between $\lambda = 0$ and 1 of almost zero, contributing little to the overall free energy change.

As a test problem, we consider the transformation of an aspartate ligand into asparagine in the active site of the enzyme aspartyl-tRNA synthetase, studied earlier with a different method discussed above.[13] The λ-dependency of the potential energy function $U(r_i;\lambda)$ is the same as before,[13] and simulations are performed for the same 11 values of λ between zero and one (see Table 1). Both the charges and the van der Waals energy terms involved in the mutation are linear functions of λ (see eq 4 and ref 13). For each value of the coupling constant λ, 30 ps of equilibration and 50 ps of data collection were performed (compared to 10 ps + 30 ps previously[13]). The finite MD simulation region has a 24 Å radius (compared to 20 Å previously). Molecular dynamics simulations were performed as described,[13] using the CHARMM program.[19] Protein atoms in the outer 4 Å were weakly restrained to their experimental positions and the water molecules were confined by a soft spherical boundary potential.[13,14] No cutoff was used for the electrostatic interactions within the simulation region. The reaction field was calculated assuming a dielectric constant of 80 for the outer region[9] and 1 for the inner region. The integration of $\partial\Delta G_{II}/\partial\lambda$ was done as before;[13] i.e., a trapezoidal method is used except at the end points, where the van der Waals contribution is fit with the theoretical $\lambda^{-3/4}$ or $(1-\lambda)^{-3/4}$ form[20] and the electrostatic term is fit using a linear response approximation. Two MD runs were performed; for the second, the system was equilibrated for an additional 30 ps before beginning the Asp → Asn transformation. The free energies to modify the outer dielectric constant were calculated with the UHBD program[21] assuming a protein dielectric constant of one, as previously.[13] A somewhat larger value of 4−6 might be more realistic, but the present assumption allows a consistent comparison with the earlier calculations. The effect on the free energy differences is expected to be small, since the dielectric screening of charges in the MD region is dominated by the high dielectric solvent portion of the outer region.

TABLE 1: Contributions to the Free Energy Derivative (kcal/mol)[a]

λ	U_{vdw}	U_{elec}	$\Delta W^0_{AB} - \Delta W^0_{AC}$	B−C coupling
0.02	26.21 (4.70)	69.04 (1.74)	85.64 (0.32)	−6.71 (0.01)
0.1	8.97 (2.99)	51.82 (9.40)	86.23 (0.53)	−6.70 (0.01)
0.2	2.39 (1.06)	33.86 (3.57)	86.23 (0.22)	−6.71 (0.00)
0.3	−3.06 (0.42)	16.19 (0.63)	86.96 (0.13)	−6.70 (0.00)
0.4	−5.08 (0.22)	7.37 (1.78)	87.03 (0.23)	−6.70 (0.00)
0.5	−5.20 (0.22)	−1.20 (2.99)	86.79 (0.19)	−6.71 (0.00)
0.6	−6.59 (0.26)	−7.57 (2.15)	86.96 (0.16)	−6.71 (0.00)
0.7	−6.51 (0.05)	−16.00 (2.21)	87.07 (0.07)	−6.71 (0.00)
0.8	−8.71 (0.20)	−37.28 (0.46)	86.49 (0.21)	−6.72 (0.00)
0.9	−10.38 (0.05)	−46.02 (0.85)	86.36 (0.12)	−6.73 (0.00)
0.98	−20.51 (0.74)	−56.33 (2.30)	86.48 (0.17)	−6.73 (0.00)

[a] Data are shown for run 1. The free energy derivative $\partial\Delta G_{II}/\partial\lambda$ is a sum over the terms listed. U_{vdw} and U_{elec} represent van der Waals and Coulombic interactions within the MD region. The next two columns are the reaction field contributions (see text). Uncertainties (in parentheses) are the standard deviation of batch means, where the data are divided into three successive batches. The last column represents the last term in eq 6 without the $(2\lambda - 1)$ factor. Multiplying by $(2\lambda - 1)$ and integrating from $\lambda = 0$ to 1, this column contributes less than 0.005 kcal/mol to the overall free energy change.

TABLE 2: Contributions to the Free Energy Change (kcal/mol)

	run 1	run 2	average
U_{vdw}	−2.35	0.08	−1.14
U_{elec}	0.65	5.82	3.24
$\Delta W^0_{AB} - \Delta W^0_{AC}$	86.62	86.53	86.58
B−C coupling	0.00	0.00	0.00
total MD step II[a]	84.91	92.43	88.67
continuum step I ($\epsilon_p \to 80$; UHBD → CHARMM)[b,c]	181.6 (0.8)	187.5 (2.5)	184.5
continuum step III (CHARMM → UHBD; $\epsilon_p \to 1$)[b,c]	−174.4 (3.7)	−181.0 (1.6)	−177.7
step I + step III	7.2 (3.8)	6.5 (3.0)	6.8
total ΔG (Asp → Asn)	92.1	98.9	95.5 (±2.8)

[a] The upper part of the table corresponds to the MD simulation step II. [b] The free energies for the continuum steps are calculated using structures from the first and last end point windows of the MD simulation; the continuum free energies are averaged over 60−70 conformations at each end point. Uncertainties for these terms (in parentheses) are estimated as the difference between the results from the first and second halves of the corresponding trajectories. [c] Includes the transformation of the outer dielectric constant, as well as the transformation between the truncated reaction potential (used in CHARMM) and the exact reaction potential (calculated by UHBD); see text.

Results and Discussion

Results for the free energy derivative $\partial\Delta G_{II}/\partial\lambda$ during the MD step II are given in Table 1; results for the total free energy change ΔG are given in Table 2. Coupling of the ligand side chains to themselves and each other contributes negligibly to ΔG ("B−C coupling" term in Tables 1 and 2). The two continuum steps I and III make large but partly canceling

contributions; their sum is 7.2 and 6.5 kcal/mol for the two runs. The total Asp → Asn free energy change is $\Delta G = 92.1$ kcal/mol for the first run and 98.9 kcal/mol for the second; the mean of the two runs is 95.5 kcal/mol. The seven earlier runs[15] with the earlier method gave similar values, ranging from 91.0 to 98.2 kcal/mol, with a mean of 95.1 ± 2.8 kcal/mol. Thus, the agreement between the two methods, which follow very different pathways between the reactant and product states, is satisfactory. Note that the Asp → Asn free energy change in solution was calculated earlier[15] and found to be about 80 kcal/mol; subtracting the free energy changes in the protein complex and in solution gives the binding free energy difference between Asp and Asn, which is thus about 15 kcal/mol.

The earlier calculations were shown to be robust with respect to the exact Asn position sampled in the product state; i.e., the Asn ligand can occupy several possible positions with similar free energies.[15] The Asn end point structure reached in the present runs is in fair agreement with, but not identical to the structures sampled during the earlier runs. The smallest rms deviation for the ligand is with the end point structure of run 6 of the earlier set (0.7 Å for run 1, 1.1 Å for run 2). The earlier run 6 gave a free energy change of 93.5 kcal/mol; see Table 2 in ref 15. Rms deviations between the end points of the seven earlier runs ranged from 1.0 to 2.7 Å.

Statistical error in $\partial\Delta G/\partial\lambda$ due to finite simulation length was shown earlier to be small;[15] a similar error level is found here for the van der Waals and Coulombic energy terms. The reaction potential contributions fluctuate little, and display a low statistical uncertainty (e.g., using only every tenth data point changes the free energy derivative contributions by less than 0.5%). The contributions of the continuum steps I and III are averaged over conformations taken from the MD simulations of the two end points of the mutation (see Table 2); they display a certain variability when the two halves of the appropriate MD windows are used ($\pm 3.0-3.8$ kcal/mol). However, the contributions from the two runs are very similar. Therefore, we can estimate the overall uncertainty of the present approach to be similar to the earlier approach (± 2.8 kcal/mol). The overall uncertainty could be lowered by performing additional runs.

The reaction potential in the MD simulations is not the exact continuum electrostatics result. The exact reaction potential can be written as a function of the protein and solvent atomic positions in the form of an infinite series of spherical harmonic functions,[22] whereas a truncated expansion (up to order 15) is used in the MD simulations.[9] This does not introduce any error into the calculated free energy ΔG, because the difference between the exact and truncated reaction potentials is included in the continuum steps I and III (Figure 1). Indeed, the free energies for these steps can be decomposed into two contributions. One corresponds to reversibly changing the truncated reaction potential into the exact reaction potential; the other corresponds to the outer dielectric change. The second contribution is small, as noted earlier:[13] changing the protein dielectric constant in the outer region from 80 to 1 contributes only -0.5 kcal/mol to ΔG. The first contribution, i.e., the difference between the truncated reaction potential (implemented in CHARMM) and the full reaction potential (calculated by UHBD), produces the remainder of the step I and III continuum contributions. If a very accurate reaction potential expansion were used in the MD simulation (at a significant additional cost), the first contribution would become small, while the free energy change for the MD step would change in a compensating manner, so that the overall free energy would in principle be the same, within statistical error. It is more efficient to use a less accurate expansion and correct for it in the continuum steps I and III.

The previous hybrid molecular dynamics/continuum electrostatics approach[13] used stochastic boundary conditions[14] for the MD simulation step; i.e., the MD model was essentially surrounded by vacuum. This leads to surface tension that increases the internal density; in the case of pure water at room temperature, for example, the increase is about 6%.[14] In the present system, most of the MD region is occupied by protein, and the protein atoms near the outer boundary are harmonically restrained to their experimental, reactant state positions, so that surface tension effects are limited. However, for other systems they could be larger, leading to structural changes when the system is transferred from bulk solvent (reactant state) to vacuum (beginning of the MD step), and from vacuum (end of the MD step) back to bulk solvent (product state). The present approach surrounds the spherical MD region with bulk continuum solvent during the MD step. This has been shown to improve the internal density and pressure significantly in the case of pure water and dilute aqueous solutions.[9] As a result, structural changes during steps I and III of the pathway are expected to be smaller, and the continuum model should perform more reliably for these steps.

In conclusion, the present hybrid molecular dynamics/continuum electrostatics approach has been shown to be efficient and reliable. It is slightly simpler to implement than the earlier hybrid approach[13] and is expected to reduce structural artifacts associated with excess density and pressure that have been observed in stochastic boundary simulations.[9,14] The physical approximations associated with the continuum model are well-defined, and the model can be improved systematically by increasing the size of the microscopic region. The moderate statistical uncertainty found here could be reduced further by performing longer end point simulations (allowing more extensive conformational averaging for the continuum steps I and III) and by performing additional runs for the alchemical mutation step II (e.g., seven runs were performed in the previous application, compared to two in this work). The method can be combined with a quantum mechanical treatment of a part of the microscopic inner region, allowing enzymatic reactions to be studied.[1,23] For a local transformation in a large protein, such as the point mutation studied here, the computational cost of the present method should be significantly less (by close to 1 order of magnitude) than an approach that uses periodic boundary conditions and Ewald summation.

Acknowledgment. A critical reading of the maniscript by A. Dejaegere and R. Stote is acknowledged.

References and Notes

(1) Warshel, A. *Computer modelling of chemical reactions in enzymes and solutions*; John Wiley: New York, 1991.
(2) Nakamura, H. *Q. Rev. Biophys.* **1996**, *29*, 1−90.
(3) Tembe, B.; McCammon, J. *Comput. Chem.* **1984**, *8*, 281−283.
(4) Warshel, A.; Sussman, F.; King, G. *Biochemistry* **1986**, *25*, 8368−8372.
(5) Brooks, C.; Karplus, M.; Pettitt, M. *Adv. Chem. Phys.* **1987**, *71*, 1−259.
(6) Hummer, G.; Pratt, L.; Garcia, A. *J. Phys. Chem.* **1996**, *100*, 1206−1215.
(7) Sakane, S.; Ashbaugh, H. S.; Wood, R. H. *J. Phys. Chem. B* **1998**, *102*, 5673−5682.
(8) Alper, H.; Levy, R. *J. Chem. Phys.* **1993**, *99*, 9847−9852.
(9) Beglov, D.; Roux, B. *J. Chem. Phys.* **1994**, *100*, 9050−9063.
(10) Gilson, M.; McCammon, J.; Madura, J. *J. Comput. Chem.* **1995**, *16*, 1081−1095.

(11) Im, W.; Beglov, D.; Roux, B. *Comput. Phys. Commun.* **1998**, *109*, 1−17.
(12) Resat, H.; McCammon, J. *J. Chem. Phys.* **1996**, *104*, 7645−7651.
(13) Simonson, T.; Archontis, G.; Karplus, M. *J. Phys. Chem. B* **1997**, *101*, 8349−8362.
(14) Brünger, A. T.; Brooks, C. L.; Karplus, M. *Chem. Phys. Lett.* **1984**, *105*, 495−500.
(15) Archontis, G.; Simonson, T.; Moras, D.; Karplus, M. *J. Mol. Biol.* **1998**, *275*, 823−846.
(16) Warwicker, J.; Watson, H. *J. Mol. Biol.* **1982**, *157*, 671.
(17) Roux, B.; Simonson, T. *Biophys. Chem.* **1999**, *78*, 1−20.
(18) Landau, L.; Lifschitz, E. *Electrodynamics of Continuous Media*; Pergamon Press: New York, 1980.
(19) Brooks, B.; Bruccoleri, R.; Olafson, B.; States, D.; Swaminathan, S.; Karplus, M. *J. Comput. Chem.* **1983**, *4*, 187−217.
(20) Simonson, T. *Mol. Phys.* **1993**, *80*, 441−447.
(21) Madura, J.; Briggs, J.; Wade, R.; Davis, M.; Luty, B.; Ilin, A.; Antosiewicz, J.; Gilson, M.; Baheri, B.; Scott, L.; McCammon, J. *Comput. Phys. Commun.* **1995**, *91*, 57−95.
(22) Jackson, J. *Classical electrodynamics*; Wiley: New York, 1975.
(23) Bash, P.; Field, M.; Karplus, M. *J. Am. Chem. Soc.* **1989**, *109*, 8092.